

PART OF A SPECIAL ISSUE ON FUNCTIONAL–STRUCTURAL PLANT MODELLING

Towards a functional–structural plant model of cut-rose: simulation of light environment, light absorption, photosynthesis and interference with the plant structure

Gerhard Buck-Sorlin^{1,2,*}, Pieter H. B. de Visser², Michael Henke⁵, Vaia Sarlikioti⁶,
Gerie W. A. M. van der Heijden¹, Leo F. M. Marcelis^{2,3} and Jan Vos⁴

¹Biometris, ²Greenhouse Horticulture, ³Horticultural Production Chains, ⁴Centre for Crop Systems Analysis, Wageningen UR, Droevendaalsesteeg 1, 6708 PB Wageningen, the Netherlands, ⁵Georg-August-University of Göttingen, Department of Ecoinformatics, Biometrics and Forest Growth, Büsgenweg 4, 37077 Göttingen, Germany and ⁶Institut National de la Recherche Agronomique, Unité de Recherches en Ecophysiologie et Horticulture, Domaine St-Paul, Site Agroparc, 84914 Avignon Cedex 9, France

* For correspondence. E-mail gerhard.buck-sorlin@wur.nl

Received: 3 March 2011 Returned for revision: 7 April 2011 Accepted: 25 May 2011

• **Background and Aims** The production system of cut-rose (*Rosa × hybrida*) involves a complex combination of plant material, management practice and environment. Plant structure is determined by bud break and shoot development while having an effect on local light climate. The aim of the present study is to cover selected aspects of the cut-rose system using functional–structural plant modelling (FSPM), in order to better understand processes contributing to produce quality and quantity.

• **Methods** The model describes the production system in three dimensions, including a virtual greenhouse environment with the crop, light sources (diffuse and direct sun light and lamps) and photosynthetically active radiation (PAR) sensors. The crop model is designed as a multiscaled FSPM with plant organs (axillary buds, leaves, internodes, flowers) as basic units, and local light interception and photosynthesis within each leaf. A Monte-Carlo light model was used to compute the local light climate for leaf photosynthesis, the latter described using a biochemical rate model.

• **Key Results** The model was able to reproduce PAR measurements taken at different canopy positions, different times of the day and different light regimes. Simulated incident and absorbed PAR as well as net assimilation rate in upright and bent shoots showed characteristic spatial and diurnal dynamics for different common cultivation scenarios.

• **Conclusions** The model of cut-rose presented allowed the creation of a range of initial structures thanks to interactive rules for pruning, cutting and bending. These static structures can be regarded as departure points for the dynamic simulation of production of flower canes. Furthermore, the model was able to predict local (per leaf) light absorption and photosynthesis. It can be used to investigate the physiology of ornamental plants, and provide support for the decisions of growers and consultants.

Key words: Cut-rose, *Rosa × hybrida*, bud break, light distribution, interactive modelling, functional–structural plant model, FSPM, L-system, virtual PAR sensor.

INTRODUCTION

Cut-rose (*Rosa × hybrida*) is an important horticultural commodity worldwide. Cut-roses are grown in greenhouses, in which most environmental factors are controlled (temperature, CO₂, supply of water and nutrients, relative humidity, light). Roses are vegetatively propagated from cuttings, which consist of a piece of stem with a leaf and an axillary bud. The cutting is rooted and the bud grows out to form the primary shoot. The primary shoot is usually prevented from flowering and bent down after 6–8 weeks. Secondary buds located in the axils of scale leaves at the base of the bent primary shoot grow out to form a number of shoots, so-called ‘bottom breaks’. After several cuts of bottom breaks and of descendant shoots (each time leaving a ‘stump’ of the harvested shoot) a ‘permanent basal structure’ of the plant is

built with axillary buds in various positions which may break to produce new ‘upright shoots’ (altogether constituting the ‘upright canopy’). The latter are harvested once a flower bud has advanced to the appropriate developmental stage. Small shoots and shoots without a flower are bent down. The bent shoots branch, forming the ‘bent canopy’ that serves to produce assimilates for ‘upright shoots’. In contrast to the upright canopy, shoots in the bent canopy are prevented from forming flowers by regular removal (‘pinching’) of flower buds. One crop produces shoots continuously over a period of 4–6 years.

Growth and development also depend on management. The latter involves harvesting time, cutting height, pruning, bending and greenhouse climate control. In the face of continuous change in technology and cultivar characteristics, there is a strong desire for an improved understanding of the

relationships between the plant's architecture, the distribution of buds (as determined by the architecture) and breaking of axillary buds as well as the quality of shoots arising from these buds, with a prerequisite for the presence of a perfect flower on the top of the stem.

Functional–structural plant models (FSPMs, also known as virtual plants) can be defined as models explicitly describing the development over time of the three-dimensional (3-D) architecture or structure of plants as governed by physiological processes which, in turn, are driven by environmental factors (Kurth, 1994; Sievänen *et al.*, 1997; Vos *et al.*, 2010). Commonly such models describe a plant as a set of interconnected phytomers. A phytomer is a growth unit resulting from the activity of an apical meristem and usually consisting of an internode, a leaf and an axillary bud. The organs of each phytomer have attributes such as weight, shape, orientation in space and optical properties that affect the amount of light intercepted, e.g. for photosynthesis. This modelling approach is particularly suited to integrate and apply knowledge on plant architecture and bud break. In particular, feedback between structure and function can be implemented and verified at various levels, e.g. locally at the organ scale and globally at the plant or canopy scale.

When designing an FSPM of a glasshouse cut-rose crop a number of elements need to be considered, including: (1) light distribution and light interception, (2) photosynthesis, (3) bud break, (4) the dynamics of growth and development of individual organs, (5) manipulation of the plant structure by cutting and bending, and (6) plant architecture.

Light distribution and light interception. Light received by individual leaves in the canopy comes from several sources: direct sunlight and diffuse sky light penetrating the cover of the glasshouse, and light from additional lamps [e.g. high-pressure sodium (SON-T) lamps] mounted in a particular configuration at some height above the canopy. Modelling entails defining the directions and flux densities from each source as these change over the course of the day. Depending on the purpose of the study a distinction can be made between receipt of total energy or only photosynthetically active radiation (PAR), while for an understanding of photomorphogenetic effects separate simulation of red and far-red radiation is required (Evers *et al.*, 2006; Kahlen and Stützel, 2011). Optical properties of the plant and glasshouse material determine the scattering of light in the canopy and the receipt of energy at each position in the 3-D structure. Buck-Sorlin *et al.* (2010) have made first steps towards the adequate modelling of these complex light regimes.

Simulation of the (daily) carbon assimilate production rate. Calculation of the production rate of carbon assimilates, or gross photosynthesis, depends on simulating the position and orientation in space of leaves, their area, photosynthetic properties and light absorption. There are various models available that calculate the leaf photosynthesis rate in rose (e.g. Lieth and Pasion, 1990; Kim and Lieth, 2003). These models can be applied at every time step to every single leaf unit that is distinguished in the 3-D model. In glasshouse production it

is important that photosynthesis models are chosen that adequately quantify the effects of variable temperature and carbon dioxide concentration as these environmental variables are subject to management.

Bud break. In principle a model needs to keep track of all buds in the plant structure. At each time step it needs to evaluate the probability of breaking of a bud, given its position and environmental parameters. Correct quantification of bud break is essential if the model is to be of value for the industry. Bud break could simply be computed as a function of the topological distance of the bud to a cutting surface, as done by Pien (2007). However, such a model can only be applied to axillary buds positioned on the stumps of harvested upright shoots ('stump buds'), as only for these are sufficient data available. There is, to our knowledge, no quantitative information about the breaking of axillary buds within the bent canopy.

Dynamics of growth and development of individual organs. Meristems produce new phytomers. The organs of a phytomer (internode, petiole, leaf blade, axillary bud) exhibit characteristic dynamics with respect to their time of initiation, their increase in weight and volume, shape and orientation in space (Fournier and Andrieu, 2000).

Plant manipulation. The fate of a rose plant is characterized by continuous human interference: bending of shoots, harvesting flower canes, pruning and 'pinching' (removal of flower-bearing branches). Each of these interferences has consequences for the functioning of the plant. For instance, taking away a flower branch also entails removal of its mature leaves, which are a source, but also alters the hormonal balances governing bud break. Hence, it is essential to develop provisions to allow interruption of the model run, to execute the type of interferences mentioned. Such interferences can be phrased as rules, which are applied either automatically and then linked to conditions, e.g. 'remove all mature shoots at a specified cutting height', or manually, executing a particular interference with an organ chosen interactively by the user. The properties of removed material such as leaf area, weight, length and diameter of harvested shoots need to be retrievable.

Plant architecture. The recurrent application of the processes described above, mainly bud break and growth and development of organs, in combination with plant manipulation, results in the architecture of the plant. This 3-D structure modifies the local light climate, thus having an influence on local light interception and photosynthesis, and ultimately on growth and development of further structures.

The objective of the present paper is to describe a static FSPM of cut-rose focusing on simulation of the local light climate and photosynthesis rate in connection with plant manipulation. We show, under different scenarios, the influence of initial plant set-up (plant density) and the history of structure management (size of the bent canopy) on light interception and canopy photosynthesis.

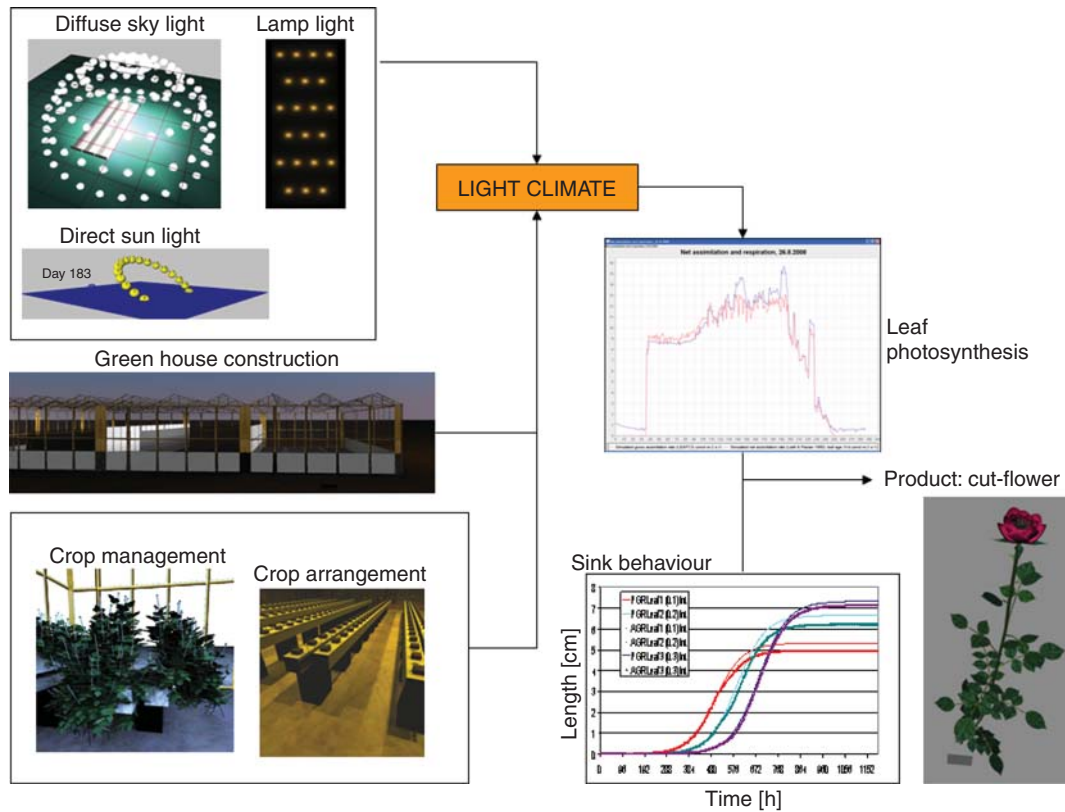


FIG. 1. Principal elements of the cut-rose FSPM, with an emphasis on light climate.

MATERIALS AND METHODS

Scope of the model

The model is based on the reconstruction of the structure of a mature cut-rose production system within a virtual greenhouse (Fig. 1). The model was written in the modelling language XL (Kniemeyer, 2008) using the open-source GroIMP platform (www.sourceforge.net/projects/groimp).

Each simulated rose plant consists of a bent shoot canopy, a framework of stumps (the ‘permanent basal structure’) and a number of upright flower shoots, formed from axillary ‘stump buds’. The root system is neglected in our model.

Light regime in the virtual greenhouse

Details of the light model used can be found in Buck-Sorlin *et al.* (2010). Essentially, an instance of the GroIMP radiation model (Hemmerling *et al.*, 2008) is invoked and carried out at each model step, computing the local PAR perception of virtual sensor objects and PAR-absorbing leaf objects in a 3-D scene. The 3-D scene consists of the virtual greenhouse with the crop and assimilation lamps (see above) inside, surrounded by sky and sun, providing diffuse and direct light, respectively. Output of both the sky and the sun are dynamic functions of the day of the year and time of the day (h). The sky is modelled as an array of 72 directional lights arranged in a hemisphere (six concentric rings each consisting of 12 lights; cf. Evers *et al.*, 2010, for a similar arrangement).

The sun object is another directional light, which dynamically changes its output like the sky object, but also its position. The position of the sun in normalized coordinates was computed as a function of day of year and time of day, following Goudriaan and van Laar (1994). Inside the greenhouse, 10 000 randomly arranged virtual spherical PAR sensors (radius 5 cm) were placed inside an invisible bounding volume (a rectangular cuboid of length 4 m, height 2 m and width 1.2 or 0.65 m in the high-density scenario) around the interior double-row of the simulated rose canopy to measure incident downward PAR in the bent and upright canopy up to a height of 2 m above the greenhouse floor. The virtual sensors are a feature of the GroIMP radiation model. They are invisible, i.e. do not interfere with the path of the rays but only measure the irradiance at their surface. Furthermore, only the upper hemisphere of a sensor is used and incoming radiation is cosine-corrected, thus making the sensor a fairly correct model of the widely used photosynthetic photon flux density (PPFD) quantum sensor. Such virtual sensors within the simulated crop allow us to establish an accurate 3-D map of the spatial light distribution. The bounding volume of virtual sensors was divided into 200 horizontal layers of 1 cm height, and the mean value of about 50 virtual sensors per layer was sampled. In addition, the amount of PAR [PPFD ($\mu\text{mol photons m}^{-2} \text{s}^{-1}$)] absorbed was computed by the light model at every step in each leaf. The radiation model itself (Hemmerling *et al.*, 2008) is an inversed Monte-Carlo raytracer (Veach, 1998). Put simply, it produces light transport

TABLE 1. Model parameters

Description	Value (range*)	Unit
Greenhouse (set-up and climate)		
Dimensions of greenhouse compartment (L, W, H)	12, 12, 5	m
Distance between gutter rows	1-2	m
Total width of double-row	0-2	m
Length of a slab	1	m
Number of plants per slab	5	–
Number of double-rows	5	–
Number of slabs per double-row	8	–
Total number of simulated plants	400	–
Height of assimilation lamps (from ground)	3-6	m
Conversion factor daylight [PAR (W) to PPFD]	4-55	$\mu\text{mol J}^{-1}$
Conversion factor SON-T lamp [PAR (W) to PPFD]	4-79	$\mu\text{mol J}^{-1}$
Spacing between lamps within the same row	2	m
Spacing between lamps in different rows	3-5	m
Daylight threshold below which assimilation lamps are switched on	200	$\mu\text{mol PAR m}^2 \text{s}^{-1}$
CO ₂ concentration in air	460	$\mu\text{mol mol}^{-1}$
Relative humidity of air	84	%
Daily mean temperature	20-5	°C
Plant architecture parameters		
LAI of bent canopy	3-0	$\text{m}^2 \text{m}^{-2}$
Default cutting height (above base of cutting)	0-1	m
Maximum phytomer rank	(19–22)	–
Leaf divergence angle	54.1 ± 16.2	°
Length of terminal leaflets	(0-0185–0-0541)	m
Width of terminal leaflets	(0-013–0-038)	m
Length of lateral leaflets	(0-02–0-044)	m
Width of lateral leaflets	(0-014–0-03)	m
Divergence angle of lateral leaflets	(55–65)	°
Form factor for leaflet area (= area/(length*width))	0-7038	–
Number of leaflets per leaf ²	{1,3,5,7}	–
Plastochron	1-5	d
Internode length [†]	(0-000012–0-0596)	m
Internode diameter	0-004–0-00015*rank	m
Phyllotactic angle	$124. \pm 39.3$	°

* A range of values is understood to follow a uniform distribution.

[†] Number of leaflets and internode length are a function of the relative acropetal rank $rr = \text{rank}/\text{maximum rank}$.

paths ('rays'), thereby connecting light sources with scene objects. The number of rays emitted by all light sources as well as the number of times a ray is followed on reflection or transmission after encountering a scene object can be determined by the user. A combination of 20 million rays and ten reflections per ray turned out to be sufficient for our purposes. Note that during one run of the radiation model, the entire scene is bombarded with rays, including the greenhouse (see Table 1 for dimensions). On average, the different elements of the greenhouse (floor, glass walls, roof) absorbed around $140 \mu\text{mol m}^{-2} \text{s}^{-1}$ of daylight (with lamps switched off), which represented about 45 % of the total light emitted by all light sources at a given moment.

The path of a ray in the scene and the likelihood with which it will be absorbed, reflected or transmitted depends on the geometry and distribution of objects in the scene as well as on their optical properties. The latter were modelled using shaders that are mapped onto the geometrical objects representing organs. In the case of leaves these were composed of a terminal leaflet and a variable number of lateral leaflet pairs, connected to each other by a midrib. For each leaflet, a parallelogram object was used, with length and width, times a form factor (Table 1), representing measured leaflet length and width, respectively. As a texture a so-called

AlgorithmSwitchShader was used (Kniemeyer, 2008), a shader with two options. For the realistic visualization of leaflets, textures were used (Figs 2 and 3). For computation of light absorption, a simple RGB shader (Kniemeyer, 2008) was employed, in which the measured diffuse reflection and transmission for the red, green and blue wavebands (600–700, 500–600 and 400–500 nm, respectively) were specified (diffuse reflection for R, G, B: 6-6, 15-2 and 1-5 %, respectively; diffuse transmission for R, G, B: 5-4, 8-6 and 4-7 %, respectively, cf. Paradiso *et al.*, 2011). The amount of PAR absorbed by a leaf, I_a , as computed by the radiation model is:

$$I_a = I_i - I_t - I_r \quad (1)$$

where I_i is the incident PAR reaching the leaf, and I_t and I_r are the amounts of transmitted and reflected PAR, respectively.

For greenhouse crops such as cut-rose, the path of the direct and diffuse light coming from the sky is further modified by the geometry and optical properties of the greenhouse (Buck-Sorlin *et al.*, 2010). The light climate inside the greenhouse was modelled by reconstructing a 3-D geometrical model of a greenhouse compartment consisting of side walls, roof and shading screens; for all of these the measured optical properties were set and the transmissivity of the textures were

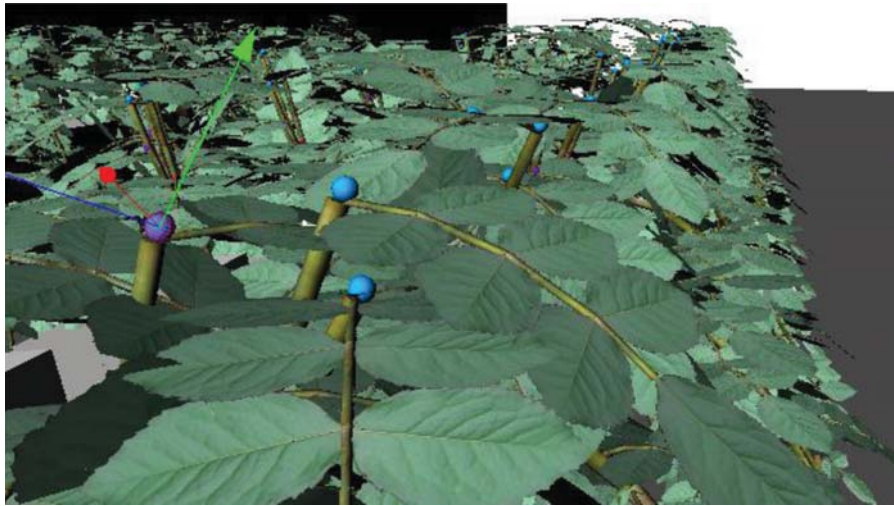


FIG. 2. Close-up of a simulated stump after flush harvest. Buds below a cut surface are marked and the first three of them are visualized as coloured spheres. Buds are assigned a proximity number (pn) and their probability for breaking is determined as a function of that number. A bud with $pn = 1$ has been selected.

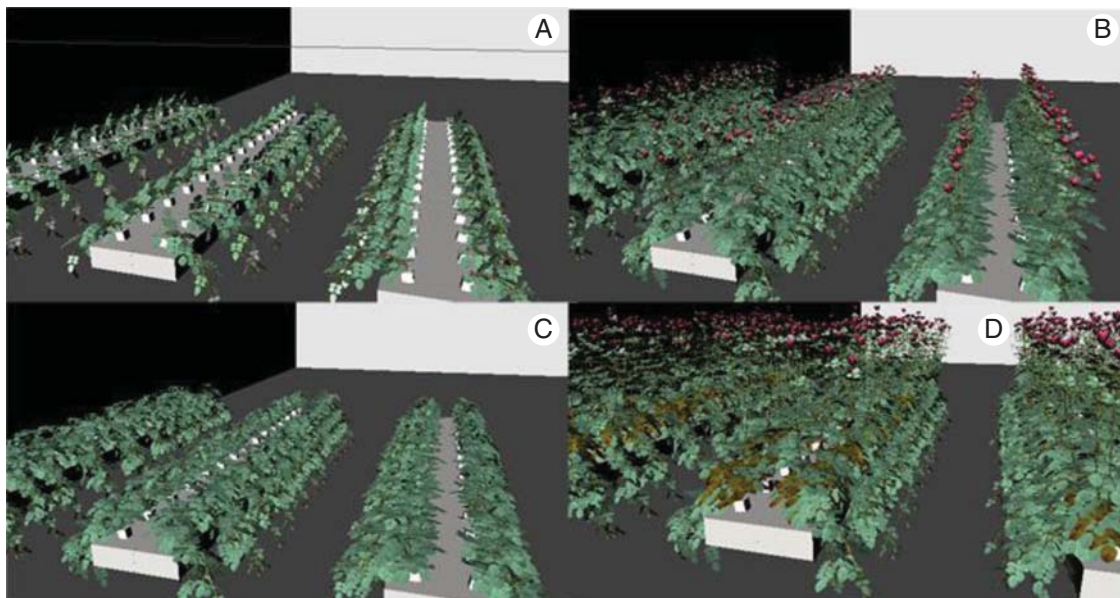


FIG. 3. Illustration of the rapid mock-up technique, showing different states of the canopy: (A) after bending of the primary shoot, (B) after creation of instant first flush, plus growth of bent canopy (branching of bent shoot, plus rebending of upright shoots), (C) after harvest of first flush and (D) second flush (note senescence of stump leaves).

calibrated to achieve an overall transmissivity of about 63% using a simulated empty greenhouse and a comparison of output of virtual light sensors placed inside and outside the greenhouse. The interior of the greenhouse compartment was reconstructed to represent the experimental set-up (see below). The virtual assimilation lamps are described in detail in Buck-Sorlin *et al.* (2010). For the lamp model, the point light object of GroIMP was extended by using measured light

distributions, thereby imitating the characteristic intensity of light emitted by the lamp in a particular direction.

Photosynthesis

Leaf photosynthesis was modelled according to the model of Kim and Lieth (2003), which is based on those of Farquhar *et al.* (1980) and Ball *et al.* (1987).

Bud break model

In the model, by default, all axillary bud objects are ranked acropetally along the shoot (i.e. numbered from rank 1 at the base to rank r_{\max} at the flower peduncle), and initially have a breaking probability of zero. Based on our observation that normally after a cutting event (harvest or pruning) on an upright shoot only the three uppermost axillary buds below the cut are breaking, with the most proximal one having the highest breaking probability and the two following buds a much lower probability, we implemented a model in which after interactive removal of shoots (see next section) the buds below the cut are marked as ‘cut’ and given a ‘proximity number’ (pn) which thus reflects the topological proximity to the cut surface (e.g. the bud below the cut has pn 1, the one below it pn 2, etc.). Breaking probability P_{BB} is then computed as an exponential function of pn , conditional on Q :

$$P_{BB} = a \cdot e^{pn \cdot b} | Q \quad (2)$$

where a and b are factors and Q is a cutting event that needs to have taken place above the bud (Fig. 2). This probabilistic bud break model is currently applied only to axillary buds on stumps, as there are no data on bud break in the bent canopy. Typical values for a and b are 4.433 and -1.564 (derived from observations in the experiment, data not shown). This resulted in bud break probabilities of 92.8, 19.4 and 4.1 % for the first three buds on the stump below the cut, and much less than 1 % for all further (i.e. lower) buds.

Interaction with the plant structure

Growers’ interactions with the plant structure is manifold but can be broken down into two main activities, namely cutting and bending. The targeted structure is generally a whole shoot (pruning and harvesting), sometimes a single organ (‘pinching’). Bending is the singular or repeated application of force to the base of a shoot with the result that the shoot will grow horizontally for a while until the tip of the shoot bends upwards again (following the natural orthotropic tendency of all rose shoots). We modelled bending in two main ways, automatic or interactive. For automatic bending a basal internode within a (primary) shoot is identified via a rule in XL, i.e.:

```
Bud (<-->) + im:Internode, rv1:RV (<-->) +
im1:Internode<r1:RL<rh:RH<(<-->){4}
rv2:RV, (im[rank]==3) ::>
{
  r1[angle]=50;
  rv1[argument]=BS;
  rv2[argument]=BS/2;
}
```

The rule identifies a sub-graph (part of the data representation of the simulated structure), consisting of an Internode named im which is accompanied by other organs (Bud, a preceding internode $im1$), with the condition that the rank of im should be 3 (i.e. the basal internode which is usually in the zone chosen for bending). In the case of interactive bending

the condition ($im[rank]==3$) on the left-hand side of the rule is replaced by another condition ($isSelected(im)$) which checks whether the internode im belonging to the sub-graph specified on the left-hand side has been selected by the user.

Harvest and pruning of shoots as well as removal of undesired flowers in the bent canopy constitute cutting, i.e. an event in which part of the structure is removed. Consider the following simplified rule:

```
x:Internode, (* x (<-->) + : (rt:Root) *),
(x.getIndiID()==rt.getIndiID() &&
x.getBent()==false &&
distance(x,rt)>=CH) ==>> cut;
```

On the left-hand side of this rule an internode x is searched for, with a context [within symbols ($* *$)] of a root rt at its base, fulfilling the following criteria: internode and root should belong to the same plant, the internode should not belong to a bent shoot, and the distance between x and rt should be bigger than a parameter CH . The effect of this query is that all upright shoots above a specified cutting height CH will be cut. This rule also marks buds below the cut (not shown) so that they can break with a specified probability (see above).

Simulation of the initial production system

For many applications it is important to explore future developments given an initial architecture. Therefore, we developed provisions allowing for the creation of an ‘instant canopy’. The number of previous flushes, the frequency, sequence, and height of harvest and pruning events will all contribute to this architecture and will equally have an influence on the following generation of harvestable shoots. By employing a ‘rapid mock-up’ technique, a specific initial production situation can be recreated. In the frame of this method an instant canopy consisting of upright shoots is produced, in which each upright shoot is created from a basal bud within one step, and consisting of the proper organs (leaves, internodes, flowers). Organ dimensions are set using stochastic variables derived from detailed measurements (Table 1) carried out in another experiment in May–July 2009, which will be described in detail in a subsequent paper. For bud break the same probabilities are applied as described above. In addition to the formation of the instant upright canopy (essentially a flush of harvest-ripe shoots) the bent canopy can be enhanced by instantly forming more lateral shoots until a user-specified leaf area index is obtained. More specifically, the uppermost ten axillary buds of the bent primary shoot break to form second-order side shoots with up to ten phytomers, which are also instantly bent down. Alternatively, the bent canopy can be reduced in size by applying a specific cutting rule. Note that these rules are simply there to design an initial structure as a departure point for subsequent simulation of shoot production but are themselves not the outcome of the feedback of photosynthesis with simulated sink functions.

Formation of an instant canopy can be achieved by combining structure formation rules in one method ‘*initialCanopy()*’, with automatic application of a specified sequence of the interaction methods described above. Thus, if it were desired to simulate the third flush of a production system, the *initialCanopy()* method could consist of the following sequence of commands:

```
buildCanopy();           pickBentFlower();
flushHarvest();         buildCanopy();
increaseCH(0.03);       flushHarvest();
buildCanopy();
```

Figure 3 illustrates the principle of the rapid mock-up technique.

Model implementation

The model consists of several modules: the main module (1) loads and initializes global parameters from external files (e.g. species- and management-specific parameters, as well as greenhouse and general climate data, see Table 1); (2) initializes environment, plant individuals and canopy; (3) controls information flow (simulates processes at different temporal resolutions for light model, photosynthesis and morphology); (4) provides interactive harvest and pruning functions (continuous or flush, Buck-Sorlin et al., 2011) that allow the user to interact with the structure at any time during the simulation; and (5) creates output files and charts. All plant organs are implemented in a Modules file. Objects are defined for different hierarchical scales, from aggregated organs such as Canopy, Individual or Shoot down to basic organs such as FlowerMeristem, Root, Leaf, Bud, Internode (including flower peduncle) and Flower, and on an even lower level Leaflet and Petiole. All basic organs, e.g. leaf, internode, root and flower, implement the same organ interface, thereby ensuring that all organ types are equipped with the same functionality and can be handled in the same straightforward way.

Experimental set-up and measurements

Experiments to collect certain parameters (including light distribution and photosynthesis rate) and data for model testing were conducted in the glasshouse compartments of Wageningen University and Research Center, Wageningen, the Netherlands (51°58'N, 5°40'E). The cultivar used in the research was a white rose, *Rosa × hybrida* ‘Akito’ (Tantau). The crop was planted in one glasshouse compartment (12 × 12 m, wall height 5 m) on 25 February 2008 in double rows at a plant density of 6.5 m⁻². Each row consisted of ten 1-m-long rockwool slabs (width 15 cm, height 7.5 cm) with a total of 50 plants. The distance between the centres of two adjacent double-rows was 0.2 m, and the path width was 1.2 m (from edge to edge of two bordering slabs). Supplementary lighting was provided in the form of 24 Hortilux HS2000 Green Power (Hortilux, Pijnacker, the Netherlands) high-pressure sodium lamps (600 W, leading to a PPFD of approx. 171 μmol m⁻² s⁻¹ at a distance of 1.2 m below the lamps, with a spacing of 3.5 × 2 m. These lamps were switched on during the day and part of the night (except between 2000 and 0300 h) when the solar PAR level

TABLE 2. Model parameters defining net photosynthesis rate (Farquhar–von Caemmerer–Berry model) of leaves at different positions in the canopy

Position	J_{\max} (μmol e ⁻ m ⁻² s ⁻¹)	V_{cmax} (μmol CO ₂ m ⁻² s ⁻¹)	V_{cmax}/J (-)	α (μmol e ⁻ μmol ⁻¹)	θ (-)
Top	178.7	78.8	0.44	0.53	0.49
Middle	126.7	54.0	0.43	0.46	0.82
Base	106.5	44.9	0.42	0.43	0.83
Light bent	102.4	45.4	0.44	0.50	0.77
Shade bent	67.0	30.5	0.46	0.38	0.56

Parameters are based on measurements made in a developed ‘Akito’ rose canopy in October 2008.

was below a threshold value (200 W m⁻²). The set temperature was 19 °C at night and 23 °C during the day, relative air humidity was approx. 75 %, and *p*CO₂ was approx. 450 μmol mol⁻¹ at night and 500 μmol mol⁻¹ during the day.

Leaf photosynthesis measurements were made with an LCpro+ Advanced Photosynthesis System (ADC BioScientific Ltd, Great Amwell, UK) between 6 and 15 October 2008. Light response curves were obtained for different leaf positions in the upright and bent canopy (Table 2) at three CO₂ concentrations (400, 600 and 800 μmol mol⁻¹) and a leaf temperature of 25 °C.

Light response curves at three external CO₂ concentrations, for different leaf positions in the canopy, were determined on plants with almost harvest-ready upright shoots from experiment 1. Details about the measurements and the key parameters can be found in Table 2. The photosynthesis model was calibrated with the measured values, by tuning the following photosynthetic parameters using a genetic algorithm (Fogel, 1998; Goldberg, 1989): maximal rate of electron transport [J_{\max} (μmol e⁻ m⁻² s⁻¹)], curvature of the light response curve [θ (-)], quantum efficiency [α (μmol e⁻ μmol⁻¹)] and maximum carboxylation rate [V_{cmax} (μmol CO₂ m⁻² s⁻¹)].

Measurements of radiation distribution in the glasshouse were made 26 September and 2 October 2008, between 1200 and 1630 h under different direct and diffuse light conditions, with or without assimilation lamps switched on, in the experimental compartment in the presence of a fully grown flower crop, using a LI-190 quantum sensor (LI-COR, Lincoln, NB, USA), which measures PAR (400–700 nm waveband).

Scenarios

We designed three different simulation scenarios for plant arrangement to test the influence of a static structure on the spatial distribution of PAR and photosynthesis. We wished to test the hypothesis put forward by rose growers that reducing leaf biomass increases light-use efficiency by improving light penetration. In rose production part of the greenhouse area is wasted either by keeping the path open or by maintaining too much biomass to sustain enough assimilate production, the latter leading to an increase in respiratory costs. Some growers are using a production system in which the roses are grown on rolling gutters, thereby eliminating walking paths

altogether, while in other companies the bent canopy is allowed to grow out to cover the entire path.

Simulation scenario 1 (control) was the reconstruction of the original measured canopy structure (Table 1), i.e. with a path width of 1.2 m, and a standard bent canopy [leaf area index (LAI) about 3.0]. In scenario 2 the control structure was used but the path between the rows was reduced from 1.2 to 0.6 m, thereby creating a completely closed simulated bent canopy with bent shoots intertwining. Plant density was thus increased from 7.14 to 12.5 m⁻² as the number of plants per slab was kept the same. In scenario 3 again the plant architecture of the control was used but with the leaf area of the bent canopy reduced in the simulation by 50 % compared with the control. This was achieved by invoking a model rule that removes part of the bent shoot above rank 7 with a probability of 85 %. The LAI of the entire simulated canopies was 4.7, 4.7 and 3.2 m² m⁻², respectively, for scenarios 1–3. Simulated plant age was 70 d at the moment that PAR absorption and photosynthesis were determined. All scenarios were carried out employing the *initialCanopy()* method, i.e. an initial structure was simply reconstructed *in silico* (based on the measurements). Hourly mean values of measured climate data (PAR, temperature; from 10-min averages) for 2 October 2008 were used, an overcast day (daily total global radiation 19.5 MJ m⁻², daily total radiation measured on the ground 7.5 MJ m⁻², average atmospheric transmissivity 0.39, total complementary radiation by lamps 4.8 MJ m⁻², average PPFD 216.4 μmol m⁻² s⁻¹), to compute instantaneous light interception and photosynthesis rate. The amount of PAR intercepted by the entire canopy was estimated as the level of PAR incident above the canopy (1.80 m above the greenhouse floor) minus the level of PAR transmitted below the bent canopy (0.30 m above the greenhouse floor). The time scheme for the simulated assimilation lamps was the same as in the experimental compartment (see above), i.e. in the model the SON-T lamps were switched on when the reading of a virtual sensor array on top of the roof of the greenhouse fell below a threshold value of 200 W m⁻².

RESULTS

Spatial distribution of PAR in the canopy

A simulated rose canopy with false colours indicating the amount of PAR absorbed per m² leaf area is shown in Fig. 4(A). The amount and distribution of PAR transmitted and incident in the same scene is represented with 10 000 randomly distributed virtual sensors (Fig. 4B). The simulated PAR levels at different heights above the ground exhibited some variation, which was due both to the stochasticity of the radiation model and the heterogeneity of the simulated canopy. Figure 5 shows a comparison of measured and simulated incident PAR values, for different heights and light regimes. The simulated canopy (age 70 d) represented the mature (pre-harvest) first flush, produced using the *instantCanopy* method (see Materials and methods), the latter using stochastic parameters based on the measured architecture. Simulated incident downward PAR values were sampled as an average of about 50 sensor readings (as described before) from a horizontal layer of the measured

height. Generally, the simulated incident PAR values within the upright canopy matched the measurements rather well (Fig. 5).

The simulated percentage absorbed PAR exhibited particular dynamics during the day in the three scenarios (Fig. 6). In the control, PAR absorption ranged between 84 and 92 %, with two clear peaks at 1000 and 1500 h, and lowest absorption was observed in the early morning and evening when light was provided by SON-T lamps only. Similar dynamics can be seen in scenario 3, where the bent canopy was reduced by 50 %, except that the PAR range was wider (80–91 %) and there was a clear difference in absorption between the control and scenario 3 during times when the SON-T lamps were the only light source. In contrast to this, in scenario 2, in which the bent canopy was completely closed due to the narrow paths, almost no PAR reached the ground, and there was no diurnal dynamics, i.e. more than 99 % of the PAR was intercepted by the canopy at all times.

According to the model, PAR levels (absorbed and transmitted) were higher in the upright than in the bent canopy (Fig. 7). In all scenarios, incident PAR above the canopy was computed at approx. 170 μmol m⁻² s⁻¹ in the morning and evening when the only light sources were the assimilation lamps, fluctuating strongly during the day, with two peaks at 0900 and 1400 h, and two dips at 1100 and 1500 h. In all scenarios, PAR levels increased in the following order: transmitted PAR below the bent canopy < PAR absorbed by bent canopy < transmitted PAR at the bottom of the upright canopy < PAR absorbed by upright canopy < incident PAR above upright canopy. Also, the sum of absorbed PAR (bent canopy and upright leaves) matched the difference between incident PAR level above the canopy and transmitted PAR level below the bent canopy, showing that there was no significant loss of PAR to other structures (e.g. benches and irrigation pipes, which have black surfaces). In scenario 2 the upright canopy was absorbing nearly the entire PAR available leaving almost nothing for the bent canopy (Fig. 7B). In the control scenario levels of PAR absorbed in the bent canopy were at all times about 20 μmol m⁻² s⁻¹ below that of the upright canopy, whereas this difference was greater (50–100 μmol m⁻² s⁻¹) and more variable in scenario 3 (Fig. 7C), due to the reduced leaf area in this scenario. In scenario 3 the amount of PAR absorbed by the bent canopy quite closely followed the level of transmitted PAR in the upright canopy. By contrast, in the control the level of transmitted PAR in the upright canopy deviated strongly (by up to 50 μmol m⁻² s⁻¹) from the amount of PAR absorbed by the bent canopy (Fig. 7A).

Profiles of transmitted and incident sensed PAR at three different times of the day (0600, 1200 and 1800 h) are shown for the three simulation scenarios in Fig. 8. PAR levels were highest and the gradient steepest at noon, peaking at about 320 μmol m⁻² s⁻¹, with diffuse daylight prevalent, whereas it was lowest and shallowest at 1800 h when the lamps were the only light sources. As expected, the incident PAR levels below the bent canopy were lowest in simulation scenario 2, in which the path was completely covered with leaves of the bent canopy. Also, along the entire profile (0–2 m above the ground) the level of transmitted PAR was about 50 μmol m⁻² s⁻¹ lower than in the

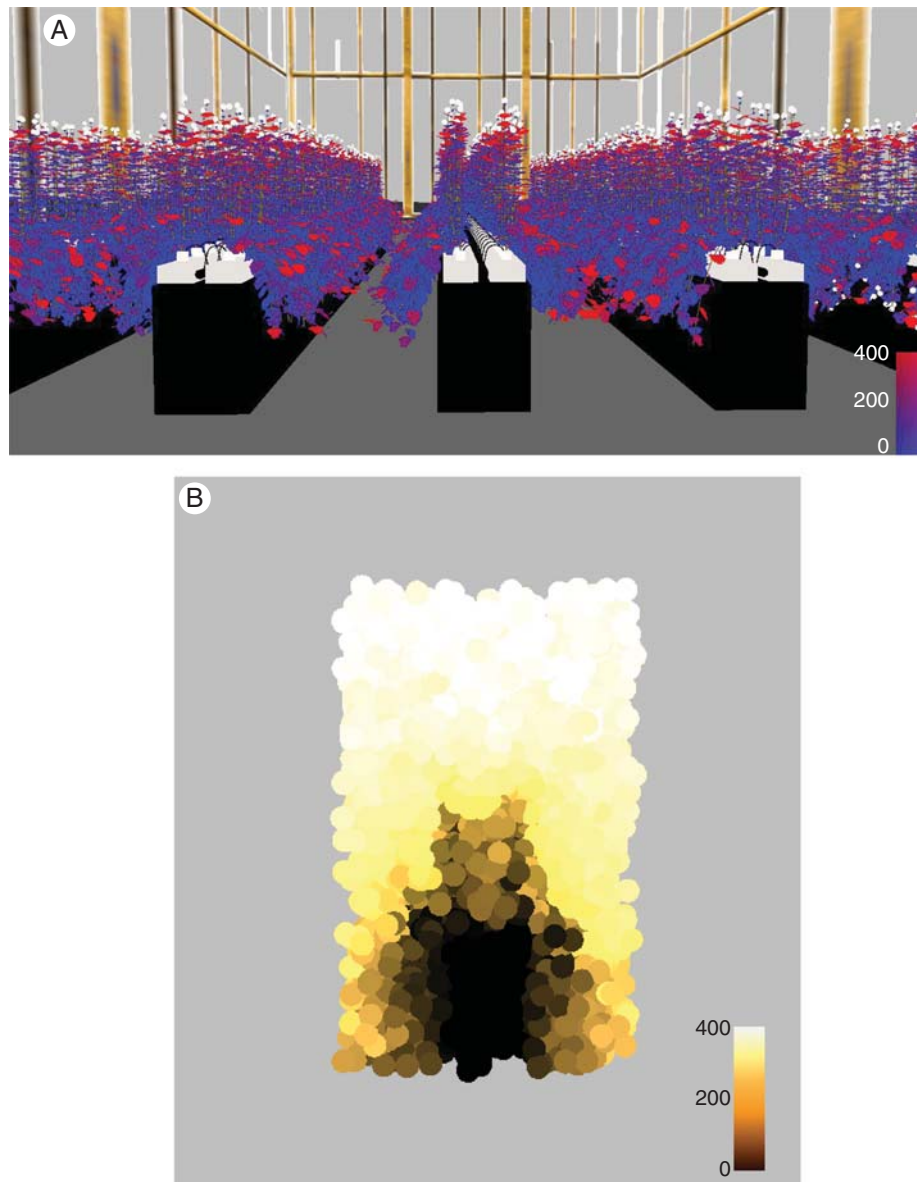


FIG. 4. Simulated rose canopy, with (A) colour gradient (blue to red) indicating increasing amount of PAR ($\mu\text{mol photons m}^{-2} \text{ leaf area s}^{-1}$) absorbed per leaf, and (B) randomly distributed virtual sensors indicating the amount of incident PAR sensed within the sensor radius (5 cm), as well as colour of incident PAR ($\mu\text{mol photons m}^{-2} \text{ sensor area}$). The snapshot shows a canopy at 1200 h, with a mixture of ambient daylight and lamp light from SON-T lamps emitting predominantly orange light.

other two simulation scenarios, due to the higher density of plants and therefore of flower canes, whereas the slopes of all gradients were equal for a given time of the day. The differences between the simulated levels of transmitted PAR in the bent canopy were rather small in the control and scenario 3 with reduced bent canopy (only about $20 \mu\text{mol m}^{-2} \text{ s}^{-1}$ at noon and $10 \mu\text{mol m}^{-2} \text{ s}^{-1}$ at the other times), with differences tending to decrease in the upper bent canopy (0.5–0.7 m above the floor).

Photosynthesis

Overall, simulated net assimilation rates of leaves of the bent and upright canopies were rather low. For leaves of

upright shoots values in the control, in scenario 2 and in scenario 3 were in the range 6–14, 10–16 and 8–14 $\mu\text{mol CO}_2 \text{ m}^{-2} \text{ s}^{-1}$, respectively, whereas in the bent canopy rates were 4–10, 2–4 and 4–8 $\mu\text{mol CO}_2 \text{ m}^{-2} \text{ s}^{-1}$, respectively. This was due to the relatively low levels of absorbed radiation. The simulated diurnal dynamics of photosynthesis closely followed that of simulated absorbed PAR, because of the linearity of the light response at these PAR levels (results not shown). In all simulation scenarios photosynthesis rates of bent shoot leaves were lower than those of leaves from upright shoots, reaching about 70 % in the control, 50–60 % in scenario 3 and only about 20 % in scenario 2, with ratios tending to increase and decrease again during the day (Fig. 9), thereby mirroring the dynamics of the PAR transmission rate in the

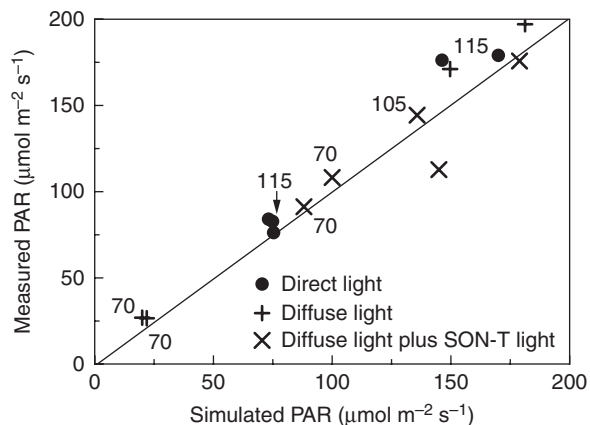


FIG. 5. Measured versus simulated incident PAR in a rose canopy. Measurements were carried out using a LI-190 quantum sensor, on 26 September (direct light) and 2 October 2008 (diffuse light) at different heights in the canopy, and at various times between 1200 and 1630 h, with varying light regimes: direct light, diffuse light, diffuse light plus SON-T light, as indicated. Numbers near the data points indicate height above the greenhouse floor at which the measurement was taken. Unlabelled data points indicate a measuring height of 130 cm (just above the canopy). Simulations are mean values from 100 randomly distributed virtual sensors, s.d. of the simulations varied between 28.7 (70 cm) and 33.0 (115 cm) $\mu\text{mol m}^{-2} \text{s}^{-1}$.

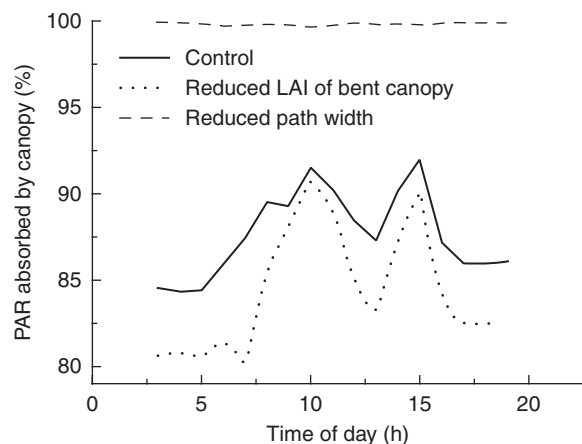


FIG. 6. Diurnal course of simulated PAR absorbed by the entire canopy, computed as $(\text{PAR}_{\text{above canopy}} - \text{PAR}_{\text{transmitted below BC}}) / \text{PAR}_{\text{above canopy}}$. Management scenarios were: control, reduced path width, and reduced LAI of bent canopy, as indicated (for more details see text).

upright canopy (Fig. 7). The very low ratio observed in scenario 2 was due to the low PAR level transmitted to the bent canopy from above through a much denser upright canopy, whereas the low ratio in scenario 3 can be explained by the reduced LAI of the bent canopy. Also, leaves in the bent canopy and the lower upright canopy exhibited a lower light response of photosynthetic rate (Table 2) than leaves from the higher upright canopy, which is another contributing factor to be taken into account when comparing photosynthetic rates of the bent and upright canopy.

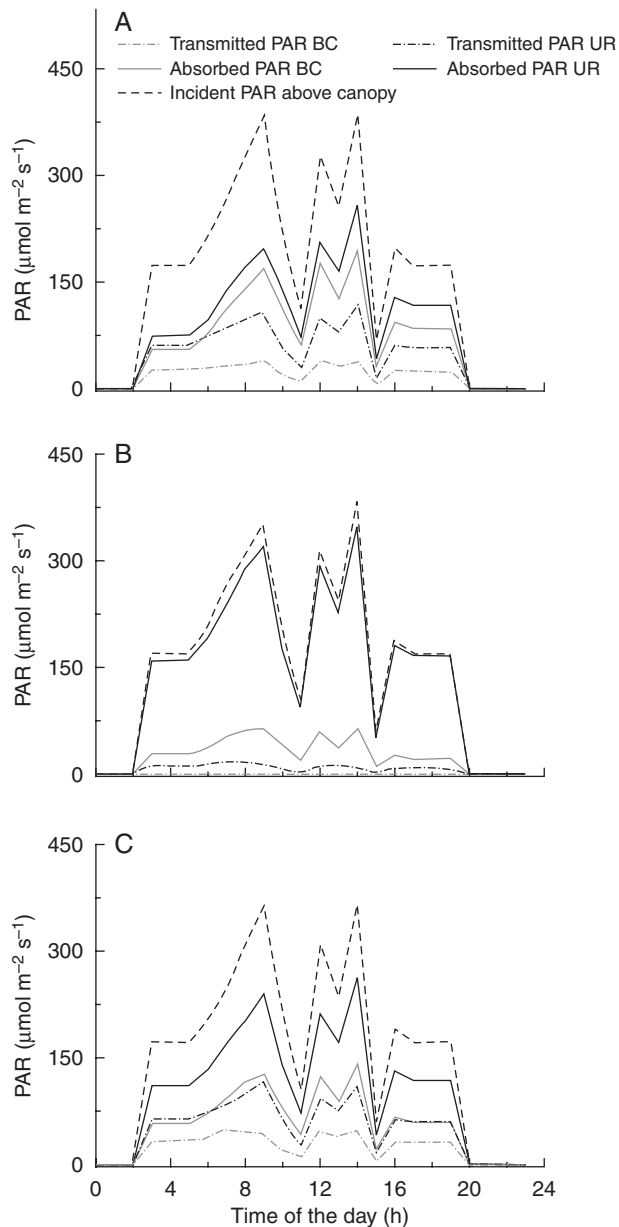


FIG. 7. Simulation of incident, absorbed and transmitted PAR levels at different heights above, inside and below a bent and upright rose canopy during the course of the day (2 October 2008). The PAR levels incident were sampled from readings of randomly distributed virtual sensors at specified heights above the floor (level incident above canopy: 1.8–1.82 m; bent canopy: 0.38–0.4 m; upright shoots: 0.7–0.72 m). Management scenarios were: (A) control, (B) reduced path width, (C) reduced LAI of bent canopy (for more details see text). BC, bent canopy; UR, upright canopy.

DISCUSSION

Light interception and photosynthesis

We chose to verify and test the plausibility of the present FSPM under local light climate, interception of PAR by leaves and local photosynthesis. Simulated local light climate, apart from being determined by greenhouse construction (e.g. transmissivity of glass), was influenced by diffuse and direct daylight as well as light coming from assimilation

lamps, all of which more or less strongly fluctuated during the course of a day. Our model was able to reproduce these dynamics in a virtual greenhouse set-up. It was equally suitable for visualizing parameters such as local PAR interception per leaf on a square-metre basis (Fig. 4A) or for generating a 3-D view of downward PAR distribution in and around a simulated canopy with the help of randomly distributed virtual sensors (Fig. 4B). Local and global light interception (per individual plant or per square metre) and subsequently local assimilate production are important drivers for shoot production (apart from the availability of buds ready to break and thus to act as sinks), and there is always potential for an

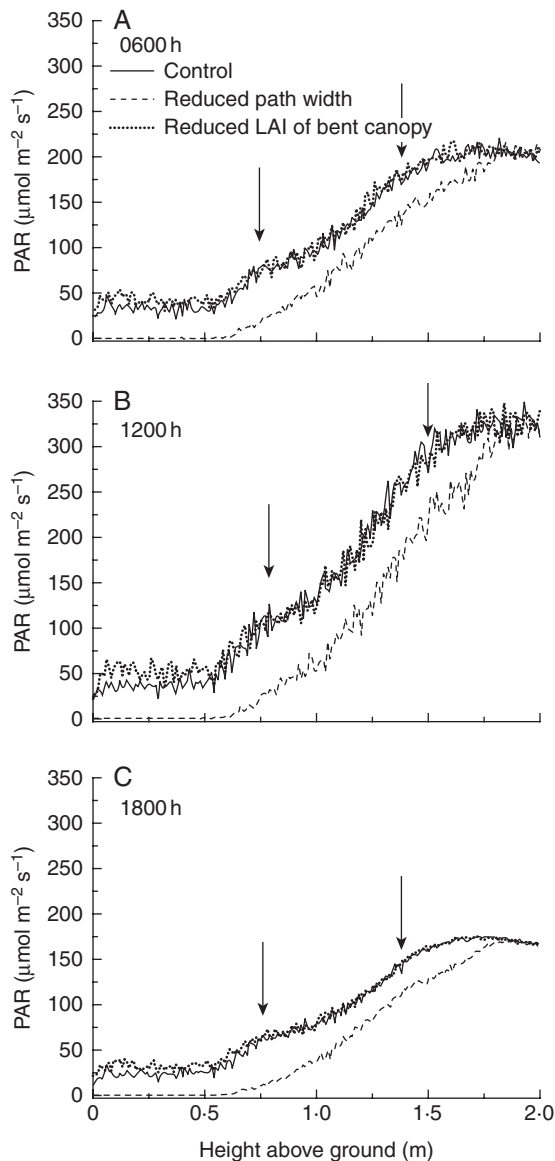


FIG. 8. Simulated PAR level at different heights and three different times of the day (0600, 1200 and 1800 h) perceived by randomly distributed virtual sensors in a simulated rose canopy, as a function of different management scenarios: control, reduced path width, and reduced LAI of bent canopy, as indicated. Arrows indicate the height of the slab and the tip of the upright canopy.

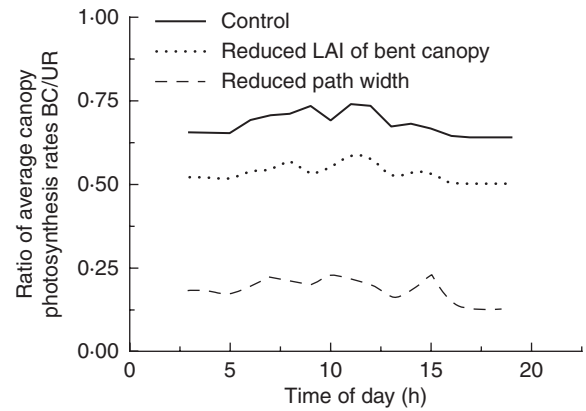


FIG. 9. Ratio between simulated net assimilation rate of leaves from upright and bent shoots during the course of one day (2 October 2008) as a function of different management scenarios: control, reduced path width, and reduced LAI of bent canopy, as indicated.

increase of source strength by optimizing management. We have shown here that the initial set-up of the producing canopy (plant density as well as extent of the bent canopy) has an effect on local light interception (with potential repercussions for photosynthesis and shoot production). The strongest effect was observed in scenario 2, in which plant density was increased from 7.14 to 12.5 m^{-2} . Light absorption of the canopy was nearly 100 %, which might mean that the density chosen for this scenario was too high. At such a rather high density one could expect feedback by the plant in the form of an altered bud break and shoot development pattern in both the bent and the upright canopy. However, such feedback is currently not implemented in our model.

A normal path width in combination with a reduced bent canopy (scenario 3) only slightly increased the level of transmitted PAR by the bent canopy (Fig. 8). This means that the amount of PAR lost to the floor (transmitted PAR below the bent canopy) was not much higher when the bent canopy was reduced, probably because the structure of the upright canopy was the same as in the control and thus the levels of transmitted PAR in the upright canopies of both control and scenario 3 were very similar. This was the impression that could be gained by analysing the sensor output only (Fig. 8). However, when comparing this with the amount of simulated PAR absorbed by the leaves of the different canopy types (bent and upright), it appears that there was a bigger difference between the control and scenario 3 with the reduced bent canopy (Fig. 7). In scenario 3 less PAR was absorbed in total, as expected, also having repercussions on the average net assimilation rate of the bent leaves (results not shown) and the ratio of assimilation rates between upright and bent shoots (Fig. 9).

The simulated diurnal curves of the incident and absorbed PAR (Fig. 7) reflected the dynamics of the light environment in the greenhouse quite accurately: during the early morning hours light came exclusively from assimilation lamps. From about 0700 h onwards the amount of (diffuse and direct) daylight was increasing, and lamps were eventually switched off once a specified threshold of external daylight was reached (as measured by virtual sensors on the roof of the greenhouse).

The rather drastic dips in simulated light levels at 1100 and 1500 h were probably due to the hourly time resolution, which did not take into account fast changes in PPFD around the threshold level, to which the lamps would react within minutes by switching on or off. The day chosen for the simulations was very overcast and therefore SON-T assimilation lamps were switched on for about 6 h, resulting in a rather typical PAR curve with a slight dip whenever lamps were switched off. Typical base values (measured and simulated in our study) were approx. $140\text{--}170\ \mu\text{mol m}^{-1}\ \text{s}^{-1}$.

Our measurements (Table 2) clearly showed that the maximum photosynthesis rate increased with increasing rank in upright shoots and from bent to upright shoots, with a clear difference between lit and shaded bent shoot leaves. Such differences in light response curves for different canopy positions were also found by [Gonzales-Real and Baille \(2000\)](#) and were ascribed by these authors to a decrease in leaf nitrogen content, i.e. the bottom leaves of the plant had 35 % less nitrogen than the top leaves. The simulated canopy photosynthesis rates obtained with our model (approx $10\text{--}12\ \mu\text{mol CO}_2\ \text{m}^{-2}\ \text{s}^{-1}$ for leaves of upright shoots, and $3\text{--}5\ \mu\text{mol CO}_2\ \text{m}^{-2}\ \text{s}^{-1}$ for leaves of bent shoots) appeared to be within the range observed by other authors ([Kim and Lieth, 2001, 2002](#)). [Kim and Lieth \(2001\)](#) found maximum rates of $13\ \mu\text{mol CO}_2\ \text{m}^{-1}\ \text{s}^{-1}$ for whole-plant net photosynthesis in the cut-rose cultivar ‘Kardinal’, whereas [Kim and Lieth \(2002\)](#), who determined the diurnal response of canopy gross photosynthesis in the same cultivar, found maximum rates of $29\ \mu\text{mol CO}_2\ \text{m}^{-2}\ \text{s}^{-1}$ for leaves of upright shoots and $24\ \mu\text{mol CO}_2\ \text{m}^{-2}\ \text{s}^{-1}$ for leaves of bent shoots on a spring day in California, with an LAI of the entire canopy of $7.6\ \text{m}^2\ \text{m}^{-2}$. However, a direct comparison with our results is difficult, given the differences in climate, cultivar and management. The model by [Kim and Lieth \(2002\)](#) is, to our knowledge, also the only one which considered – in a simplified way and still in the frame of a process-based model – the structure of the upright and bent canopy and their influence on the distribution of incident PAR, thereby also distinguishing between north–south and east–west row directions. [Sarlikioti et al. \(2011\)](#) modelled plant architecture traits and row structure, light interception and canopy photosynthesis in an FSPM of tomato and found that, in particular, the explicit description of leaf divergence angles significantly improved the prediction of canopy photosynthesis compared with an unstructured process-based model considering the Beer–Lambert law of light absorption as a function of cumulative LAI alone.

Computational cost of running the light model

To compute the local light environment around the rose canopy in the virtual greenhouse we used the built-in radiation model of GroIMP. This model is based on a unidirectional Monte-Carlo raytracer, i.e rays are traced from a light source in one direction to an object in a scene. Such models are stochastic and computationally expensive, because a large number of rays (several millions) and their fate (paths of reflection and transmission until final absorption by a medium) have to be traced in order to gain a reliable estimate of locally absorbed and available light. As an example,

consider the computational cost to run the scenarios presented here. For most of the computations, we used a Dell Precision WorkStation T7500, running an Ubuntu Linux operating system, which supported symmetric multi-processing. This workstation had a total of eight CPUs (four cores per CPU, two threads per core), a clocking rate of 2.4 GHz and 12 GB RAM. The GroIMP platform was running on a 64-bit server Java Virtual Machine. In all three scenarios, the scene comprised approx. 145 000 plant objects (48 900 leaves and internodes each and 45 600 buds) and 97 light sources (24 lamps, 72 diffuse and one direct). One model step involved the built-up of the entire canopy consisting of 400 plants and one run of the light model. Per scenario, 18 hourly steps were computed. All scenarios were computed using the so-called headless mode of GroIMP, which allowed the platform to be run without a graphical user interface from a batch file. Computation times varied among the scenarios, 1 h for the control and for scenario 2 and 50 min for scenario 3 (reduced bent canopy), or on average 2.8 and 3.5 min per step, respectively.

Further applications of the model

We also tested the influence of cutting height in another set of simulation runs (results not shown), taking the control set-up (scenario 1) as a starting point and varying the height at which the first flush of upright shoots was cut. This cutting height was defined as the distance of a point on the stump to the base of the stump (see Materials and methods). Four cutting heights were tested, 0.15, 0.2, 0.25 and 0.3 m, and an entire canopy was simulated with a mature second flush of upright shoots present (simulated plant age about 110 d). Both PAR absorbed and net assimilation rates tended to be highest at a cutting height of 0.2 m (results not shown), but the effect was not significant. It remains to be further investigated by modelling and experimentation if canopy management in terms of varying the cutting height of harvested shoots does noticeably influence light interception.

Bud break

Bud break in cut-rose is due to a complex variety of external and internal factors, such as: apical dominance and modifying factors, e.g. light [directly or through its effect on source strength ([Marcelis-van Acker, 1994a](#))]; the position of the buds along the shoot ([Marcelis-van Acker, 1994b](#)) in one of the three zones, namely basal, median or subapical ([Khayat and Zieslin, 1982](#); [Zamski et al., 1985](#)); and manipulation (pruning, ‘pinching’) and initial crop management (planting density; [Kool and Lenssen, 1997](#); [Burema et al., 2010](#)). The two basic mechanisms underlying bud break are essentially developmental ‘readiness’ of the bud and lack of correlative inhibition ([Zieslin and Halevy, 1978](#); [Khayat and Zieslin, 1982](#); [Marcelis-van Acker, 1994b](#)). In our model we used the general observations ([Pien, 2007](#)) that (1) bud break of axillary buds on stumps of harvested upright shoots was induced by cutting (harvest or pruning) of (flowering) upright shoots, probably by lifting the correlative inhibition exerted by the terminal bud or growing shoot that was

removed, and (2) that after lifting of correlative inhibition the first bud below the cut broke with a high probability and the following with much lower probability, suggesting that the shoot emerging from the uppermost bud rapidly inhibits its subjacent neighbours.

Cultivars clearly differ in frequency of bud break, i.e. the probabilities of the top, second or third bud below a cut surface breaking. One of the future promises of this model is to explore the consequences of bud break behaviour in terms of numbers of flower shoots produced and their quality (length, diameter of stem and flower bud).

Once a bud is broken and a shoot begins to develop, this will not only change the local light climate but also shift the source/sink balance, by increasing demand. Results from our own experiments (data not shown) suggest that the local level of incident PAR perceived by an unbroken bud, in combination with the number of competing sinks, influences the total number of buds breaking per shoot stump, per plant or per square metre. As the present model is completely object-oriented and modular it will be very straightforward to incorporate new processes reflecting mechanisms of bud break.

Conclusions and outlook

The model of cut-rose presented here allowed the creation of a wide range of initial structures thanks to simple interactive rules for pruning, cutting and bending. We used the structures generated to show that we can model the distribution in the canopy of light from a complex radiation environment, consisting of the solar track and the virtual glasshouse with a particular configuration of lamps. Our simulation results showed that, with respect to light interception, the bent canopy appeared to play a less important role than had been expected. Carbon assimilation per leaf, using a biochemical photosynthesis rate model, followed from local light distribution.

The implementation of dynamic concepts for source–sink relationships, bud break and phytomer growth to predict shoot production will contribute to gaining new insight into mechanisms of cut-rose physiology and in particular bud break and thus lead to a better comprehension of these mechanisms.

ACKNOWLEDGEMENTS

We thank Heiner Lieth for highly fruitful discussions about all aspects of cut-rose modelling and cultivation. We further thank the members of the users' panel for helpful discussions, in particular Ep Heuvelink, Dick van der Sar, Sjaak van der Hulst and Joop van den Nouweland. Anonymous reviewers made very valuable comments to a previous version of the manuscript. Hortilux (Pijnacker, the Netherlands) provided technical information on SON-T GreenPower lamps. Margreet Bruins, Gerard Brouwer, Jos Kanne, Johan Steenhuizen and Theo Damen provided excellent technical assistance. Benno Burema, Robert C. Okello Ongom, Alena Senkyrikova, Alisa Shlyuykova and Yanru Song helped with the experimental work. This work was supported by the Dutch Technology Foundation STW (project 07435), which is the applied science division of NWO, and the Technology Programme

of the Ministry of Economic Affairs, Product Board for Horticulture (project PT 13098) and TTI Green Genetics.

LITERATURE CITED

- Ball JT, Woodrow IE, Berry JA. 1987.** A model predicting stomatal conductance and its contribution to the control of photosynthesis under different environmental conditions. In: Biggins J, ed. *Progress in photosynthesis research*, Vol. 4. Dordrecht: Nijhoff Publishers, 221–224.
- Buck-Sorlin GH, Hemmerling R, Vos J, de Visser PHB. 2010.** Modelling of spatial light distribution in the greenhouse: description of the model. In: Li B, Jaeger M, Guo Y, eds. *Plant growth modeling, simulation, visualization and applications, Proceedings – PMA09*. IEEE Computer Society Conference Publishing Services, 79–86.
- Buck-Sorlin GH, Burema B, Vos J, Heuvelink E, Lieth JH, de Visser PHB, Marcelis LFM. 2011.** A Functional-structural plant model for cut-roses – new techniques for modelling manipulation of plant structure. In: Dorias M, ed. *Proceedings of the International Symposium on High Technology for Greenhouse Systems: GreenSys2009*. *Acta Horticulturae* **893**: 705–711.
- Burema BS, Buck-Sorlin GH, Damen T, Vos J, Heuvelink E, Marcelis LFM. 2010.** Cut-rose production in response to planting density in two contrasting cultivars. *Acta Horticulturae* **870**: 47–54.
- Evers JB, Vos J, Andrieu B, Struik PC. 2006.** Cessation of tillering in spring wheat in relation to light interception and red : far-red ratio. *Annals of Botany* **97**: 649–658.
- Evers JB, Vos J, Yin X, Romero P, van der Putten PEL, Struik PC. 2010.** Simulation of wheat growth and development based on organ-level photosynthesis and assimilate allocation. *Journal of Experimental Botany* **61**: 2203–2216.
- Farquhar GD, von Caemmerer S, Berry JA. 1980.** A biochemical model of photosynthetic CO₂ assimilation in leaves of C3 species. *Planta* **149**: 78–90.
- Fogel DB. 1998.** *Evolutionary computation: the fossil record*. New York: IEEE Press.
- Fournier C, Andrieu B. 2000.** Dynamics of the elongation of internodes in maize (*Zea mays* L.): analysis of phases of elongation and their relationships to phytomer development. *Annals of Botany* **86**: 551–563.
- Goldberg DE. 1989.** *Genetic algorithms in search optimization and machine learning*. Addison Wesley.
- Gonzales-Real MM, Baille A. 2000.** Changes in leaf photosynthetic parameters with leaf position and nitrogen content within a rose plant canopy (*Rosa hybrida*). *Scientia Horticulturae* **46**: 109–128.
- Goudriaan J, van Laar HH. 1994.** *Modelling potential crop growth processes*. Dordrecht: Kluwer Academic Publishers.
- Hemmerling R, Kniemeyer O, Lanwert D, Kurth W, Buck-Sorlin GH. 2008.** The rule-based language XL and the modelling environment GroIMP illustrated with simulated tree competition. *Functional Plant Biology* **35**: 739–750.
- Kahlen K, Stützel H. 2011.** Modelling photo-modulated internode elongation in growing glasshouse cucumber canopies. *New Phytologist* **190**: 697–708.
- Khayat E, Zieslin N. 1982.** Environmental factors involved in the regulation of sprouting of basal buds in rose plants. *Journal of Experimental Botany* **33**: 1286–1292.
- Kim S-H, Lieth JH. 2001.** Modeling diurnal variation of whole-plant photosynthesis of greenhouse roses. *Acta Horticulturae (ISHS)* **547**: 111–119.
- Kim S-H, Lieth JH. 2002.** Modeling photosynthesis of heterogeneous rose crop canopies in the greenhouse. *Acta Horticulturae (ISHS)* **593**: 121–128.
- Kim S-H, Lieth JH. 2003.** A coupled model of photosynthesis, stomatal conductance and transpiration for a rose leaf (*Rosa hybrida* L.). *Annals of Botany* **91**: 771–781.
- Kniemeyer O. 2008.** *Design and implementation of a graph grammar based language for functional–structural plant modelling*. PhD thesis, BTU Cottbus, Germany. Available at <http://opus.kobv.de/btu/volltexte/2009/593/>
- Kool MTN, Lenssen EFA. 1997.** Basal shoot formation in young rose plants. Effects of bending practices and plant density. *Journal of Horticultural Science* **72**: 635–644.
- Kurth W. 1994.** Morphological models of plant growth. Possibilities and ecological relevance. *Ecological Modelling* **75/76**: 299–308.

- Lieth JH, Pasian CC. 1990.** A model for net photosynthesis of rose leaves as a function of photosynthetically active radiation, leaf temperature, and leaf age. *Journal of the American Society for Horticultural Sciences* **115**: 486–491.
- Marcelis-van Acker CAM. 1994a.** Effect of assimilate supply on development and growth potential of axillary buds in roses. *Annals of Botany* **73**: 415–420.
- Marcelis-van Acker CAM. 1994b.** *Axillary bud development in rose*. PhD thesis, Wageningen UR, the Netherlands.
- Paradiso R, Meinen E, Snel JFH et al. 2011.** Spectral dependence of photosynthesis and light absorbance in angle leaves and canopy in rose. *Scientia Horticulturae* **127**: 548–554.
- Pien H. 2007.** *Development of a carbon allocation and growth model for a bent rose canopy*. PhD thesis, Ghent University, Ghent, Belgium.
- Sarlikioti V, de Visser PHB, Marcelis LFM. 2011.** Exploring the spatial distribution of light interception and photosynthesis of canopies by means of a functional–structural plant model. *Annals of Botany* **107**: 875–883.
- Sievänen R, Mäkelä A, Nikinmaa E, Korpilahti E. 1997.** Special issue on functional–structural tree models, Preface. *Silva Fennica* **31**: 237–238.
- Veach E. 1998.** *Robust Monte Carlo methods for light transport simulation*. PhD thesis, Stanford University, CA.
- Vos J, Evers JB, Buck-Sorlin GH, Andrieu B, Chelle M, de Visser PHB. 2010.** Functional–structural plant modelling: a new versatile tool in crop science. *Journal of Experimental Botany* **61**: 2101–2115.
- Zamski E, Oshri S, Zieslin N. 1985.** Comparative morphology and anatomy of axillary buds along a rose shoot. *Botanical Gazette* **146**: 208–212.
- Zieslin N, Halevy AH. 1978.** Components of axillary bud inhibition in rose plants. 2. Effect of stem orientation and changes of bud position on the stem by budding. *Botanical Gazette* **139**: 60–63.